Dual Cationic-Anionic Profiling of Metabolites in a Single Embryonic Cell in a Live Xenopus laevis Embryo by Microprobe CE-ESI-MS

SCHOLARONE™
Manuscripts

Dual Cationic-Anionic Profiling of Metabolites in a Single Identified Cell in a Live *Xenopus laevis* Embryo by Microprobe CE-ESI-MS

Erika P. Portero and Peter Nemes*

Department of Chemistry & Biochemistry, University of Maryland, College Park MD 20742

Correspondence to: Peter Nemes, Department of Chemistry & Biochemistry, University of

Maryland, 8051 Regents Drive, College Park, MD 20742, USA. Phone: (1) 301-405-0373.

E-mail: nemes@umd.edu.

Keywords: single-cell analysis, mass spectrometry, capillary electrophoresis, metabolomics,

Xenopus laevis

ABSTRACT

In situ capillary microsampling with capillary electrophoresis (CE) electrospray ionization (ESI)

mass spectrometry (MS) enabled characterization of cationic metabolites in single cells in

complex tissues and organisms. For deeper coverage of the metabolome and metabolic networks,

analytical approaches are needed that provide complementary detection for anionic metabolites,

ideally using the same instrumentation. Described here is one such approach that enables

sequential cationic and anionic (dual) analysis of the same identified cell in a live vertebrate

embryo. A calibrated volume was microaspirated from the animal-dorsal cell in a live 8-cell

embryo of *Xenopus laevis*, and cationic and anionic metabolites were one-pot microextracted

from the aspirate, followed by CE-ESI-MS analysis of the same extract. A laboratory-built CE-

ESI interface was reconfigured to enable dual cationic-anionic analysis with ~5–10 nM (50–100

amol) lower limit of detection and capability for quantification. To provide robust separation and

efficient ion generation, the CE-ESI interface was enclosed in a nitrogen gas filled chamber, and

the operational parameters were optimized for the cone-jet spraying regime in both the positive

and negative ion mode. A total of ~250 cationic and ~200 anionic molecular features were

detected from the cell between m/z 50–500, including 60 and 24 identified metabolites,

respectively. With only 11 metabolites identified mutually, the duplexed approach yielded

complementary information on metabolites produced in the cell, which in turn deepened network

coverage for several metabolic pathways. With scalability to smaller cells and adaptability to

other types of tissues other models, dual cationic-anionic detection with *in situ* CE-ESI-MS

opens a door to better understand cell metabolism.

INTRODUCTION

Single-cell mass spectrometry (MS) provides a molecular snapshot to investigate the phenotypical and physiological state of a cell;[1] the technology is qualitative, capable of label-free detection, and can be made quantitative. As a downstream product of transcription and translation, the metabolome, comprising of all metabolites produced by a cell, responds dynamically and rapidly to intrinsic and extrinsic events to the cell. Therefore, the single-cell metabolome raises a new frontier in the study of molecular events underlying cell differentiation and the establishment of cell-to-cell differences (cell heterogeneity) during normal and impaired development.

Detection of the single-cell metabolome presents grand analytical challenges for MS. The metabolome encompasses vast molecular complexity and spans a broad dynamic range of concentration. For example, the Human Metabolome Database (HMDB)[2] currently reports ~114,100 metabolite entries with endogenous concentrations ranging from <1 nM to millimolar concentration. Metabolites also occupy a broad spectrum of physiochemical properties[1] (e.g., pK_a and hydrophobicity) and can change rapidly (e.g., in seconds–milliseconds). In addition, cells contain substantially smaller amounts of material than typically measured by MS. Other challenges arise from varying dimensions as cells develop and different physical and temporal positions that they assume in tissues and developing organism. For example, blastomeres become progressively smaller and undergo long-range movements during morphogenesis in vertebrate embryos.[3] To better understand cell metabolism, specialized approaches are required that integrate spatially and temporally scalable sample collection, particularly in complex tissues and organisms, with trace-sensitive MS for broad types of metabolites.

These analytical challenges stimulated the development of specialized technologies and

methodologies in single-cell MS. A detailed overview of this field is available in recent reviews

(see references [1, 4-10]). Ablation/desorption by focused laser light[10] or direct aspiration using

microfabricated capillaries[11-14] extended the capabilities of single-cell MS to single cells in

isolated or complex tissues. Chemical separation prior to ionization and MS effectively increased

metabolomic coverage by minimizing ionization and spectral interferences as well as facilitating

molecular identifications by providing separation time, a compound-dependent information.

With high separation performance and a compatibility to volume-limited samples, capillary

electrophoresis (CE) found a niche in qualitative and quantitative metabolomics for single cells.

The integration of CE with matrix-assisted laser desorption ionization (MALDI) recently enabled

high-throughput screening of single-cell metabolism in pancreatic islets.[15]

We and others custom-built microanalytical CE-ESI platforms capable of low nanomolar

sensitivity (tens of attomoles). These instruments enabled the profiling of ~40 identified

metabolites in single neurons from *Aplysia californica* [16-18] and rat [18, 19] as well as ~80 identified

metabolites in single embryonic cells in 8-[13, 20, 21], 16-[13, 22], and 32-cell[13] embryos of *Xenopus*

laevis, the South African clawed frog. Furthermore, to enable spatially and temporally resolved

single-cell analysis in live developing *X. laevis* embryos[13] (see protocol in reference [23]), we

recently integrated microprobe sampling with CE-MS. However, limited ESI stability in the

negative ion mode so far curtailed single-cell CE-MS studies to cationic metabolites. Deeper

coverage of the single-cell metabolome would benefit from combined analysis of cationic and

anionic species.

Recent developments in CE-MS technology raise a potential toward anionic metabolomics

in single cells (see reviews in references [24-27]). Low limits of detections (~10–200 nM) and high

measurement reproducibility were accomplished for anions from metabolite standards and extracts of tissues and biological fluids using CE-MS interfaces that employ sheathflow[28, 29], low-flow electrokinetically-pumped[30, 31], and sheathless[32] interface designs. Nucleotides were most recently profiled in single neurons from *Aplysia californica* using a coaxial sheath-flow CE-ESI interface.[28] In principle, the combination of cationic and anionic analysis holds the potential to deepen metabolic coverage in single cells. However, individual cells contain prohibitively limited amounts of materials for independent sample processing that is typical for cationic and anionic analysis. Additionally, complex CE-ESI interface designs and the use of different CE capillaries for cationic and anionic measurements (e.g., coated capillaries) lower analytical throughput, hindering the analysis of multiple single cells to facilitate results interpretation.

Described here is a simplified methodology that enables the dual analysis of cationic and anionic metabolites in single cells of live embryos. We used capillary microsampling to collect cell material from identified single cells in live *X. laevis* embryos, which was followed by a one-pot micro extraction of anionic and cationic metabolites from the collected material. A custom-built sheath-flow CE-ESI interface was supplemented with a nitrogen gas filled environmental chamber to minimize electrical discharges at the electrospray emitter to ensure stable and efficient ion generation for detection. Cationic and anionic analysis using the same bare fused silica capillary with different electrolytes provided complementary metabolite identifications, yielding a deeper coverage of metabolic networks than was feasible using each approach in isolation using single-cell CE-ESI-MS.

EXPERIMENTAL

Chemicals. LC-MS grade solvents and chemicals including formic acid, ammonium bicarbonate, methanol, acetonitrile, isopropanol, and water were purchased from Fisher Scientific (Fair Lawn, NJ), unless otherwise noted. Trizma hydrochloride and trizma base were obtained from Sigma Aldrich (Saint Louis, MO). Cysteine was from MP Biomedicals (Solon, OH).

Solutions. Steinberg's solution (100% v/v) and cysteine solution (2% v/v) were prepared following standard protocols.[3] The "*metabolite extraction solvent*" consisted of 40% (v/v) methanol and 40% (v/v) acetonitrile (pH 4.7). For cationic analysis, the CE "*background electrolyte*" (BGE) solution was 1% (v/v) formic acid (pH 2.8) and the electrospray sheath solution was 50% (v/v) methanol containing 0.1% (v/v) formic acid. For anionic analysis, the BGE was 20 mM ammonium bicarbonate (pH 8.2), and the electrospray sheath solution was 0.2 mM ammonium bicarbonate in 50% (v/v) isopropanol.

Animal Care and Embryo Collection. All protocols regarding the humane care and handling of animals were approved by the University of Maryland Institutional Animal Care and Use Committee (IACUC no. R-DEC-17-57). Male and female adult *Xenopus laevis* frogs were purchased from Nasco (Fort Atkinson, WI) and maintained in a breeding colony. Embryos were obtained via gonadotropin-induced natural mating following established protocols.[3] The jelly coating of freshly laid embryos was removed as described elsewhere.[33] Dejellied embryos were transferred to a Petri dish containing 100% Steinberg's solution (SS). Two-cell stage embryos showing stereotypical pigmentation patterns[34] across the dorsal-ventral and left-right axis were cultured in 100% SS to the 8-cell stage for this study.

Single-cell Sampling and Metabolite Extraction. The left animal-ventral (V1) cell was identified in 8-cell embryos in reference to established cell-fate maps.[35] An ~10 nL of cellular

content was aspirated from the cell using microcapillary sampling following our recent

protocols.[13, 23] To extract small polar metabolites from the aspirate, the sample was expelled into

4 µL of *metabolite extraction solution* at ~4 °C and vortex-mixed for ~1 min at room

temperature before centrifugation at $8,000 \times g$ for 5 min at 4 °C to pellet cell debris. Metabolite

extracts were stored together with the cell debris at −80 °C until CE-ESI-MS analysis.

Single-cell CE-ESI-MS. Single-cell metabolite extracts were measured using a laboratory-

built microanalytical CE-ESI system coupled to a quadrupole time-of-flight mass spectrometer

(Impact HD, Bruker Daltonics, Billerica, MA), following our established protocols.[13, 22, 23] In this

study, CE separation was performed in a 1-meter long bare fused silica capillary with 40/105 µm

inner/outer diameter (Polymicro Technologies, Phoenix, AZ) with the outlet end grounded using

a custom-built co-axial sheath-flow CE-ESI interface[18]. Cationic analysis implemented the

following parameters: CE separation at +20–22 kV (applied to capillary inlet) in 1% formic acid

(yielding ~7.5–8 µA CE current); CE-ESI interface operated in the cone-jet regime (0.1% formic

acid in 50% methanol supplied at 1 µL/min as sheath flow) at −1,700 V spray potential applied

to mass spectrometer front plate; CE-ESI environmental chamber, no nitrogen supplied (ambient

air as bath gas). Anionic analysis was performed using the following settings: CE separation at

+17–19 kV (applied to capillary inlet) in 20 mM ammonium bicarbonate (yielding 4.9–5.6 µA

CE current); CE-ESI interface operated in the cone-jet electrospray regime (0.2 mM ammonium

bicarbonate in 50% isopropanol supplied at 0.6 µL/min as sheath) at +2,100 V spray potential

applied to the mass spectrometer front plate; CE-ESI environmental chamber, nitrogen supplied

at 0.6 L/min. In both cationic and anionic measurements, the stability of the CE-ESI interface

was characterized by ion current measurements using a mass spectrometer and by direct optical

inspection of the electrified liquid meniscus using a stereomicroscope (40× magnification,

Simul-Focal Stereomicroscope, United Scope, Irvine, CA). Identification of the electrospray regimes was performed as detailed elsewhere.[36]

Ions generated by CE-ESI were detected using a quadrupole time-of-flight mass spectrometer (Impact HD, Bruker). Experimental settings were the following: MS survey scan rate, 2 Hz; mass range (MS^1 and MS^2), *m/z* 50–550; collision-induced dissociation, 18–20 eV in nitrogen collision gas; dry gas, nitrogen at 2 L/min at 100 °C for positive and 150 °C for negative ionization mode. The mass spectrometer was externally mass-calibrated to <5 ppm accuracy by analyzing 150 mM sodium formate using CE-ESI in the positive ion mode and directly infusing 10 mM sodium formate (in 0.2 mM ammonium bicarbonate prepared with 50% v/v isopropanol) through the CE-ESI interface in the negative ion mode.

Data Analysis. Raw MS-MS/MS data were processed using a custom-written script in Compass DataAnalysis version 4.3 (Bruker Daltonics) as described elsewhere.[22] Briefly, each file was externally calibrated to <1 ppm accuracy (enhanced quadratic calibration mode) for sodium formate cluster ions that were formed in the ion source as salts separated from the samples, molecular features were semi-manually surveyed between *m/z* 50–550 with 5 mDa increments, and the resulting accurate *m/z* and migration time information was recorded for each detected molecular feature. Under-the-curve peak areas and signal-to-noise (signal/noise) ratios were calculated using Compass 4.3 (Bruker Daltonics). Metabolic pathway analysis was performed in MetaboAnalyst 4.0[37] using the Kyoto Encyclopedia of Genes and Genome (KEGG) metabolomic knowledgebase (www.genome.jp/kegg) with the following settings: Pathway library, *Danio rerio* (zebrafish); pathway analysis algorithms, overrepresentation analysis by hypergeometric test and pathway topology analysis by relative betweenness centrality.

Study Design. To account for biological variability, a total of N = 4 different V1 cells were

analyzed in this study, each from a different embryo from a different clutch over a three-month

period. For each cell, dual cationic-anionic analysis was performed in technical duplicate–

triplicate.

Safety Considerations. Standard safety procedures were followed when handling chemicals

and biological samples. Capillary micropipettes and electrospray emitters, which pose a potential

puncture hazard, were handled with gloves and safety goggles. To prevent against electrical

shock hazard posed by high voltage, all electrically connective parts of the CE-ESI setup were

earth-grounded and isolated in an enclosure equipped with a safety interlock-enabled door.

RESULTS AND DISCUSSION

Technology Development. The goal of this study was to enhance the characterization of

small polar metabolites in single cells, specifically in identified blastomeres directly in live

embryos. We recently adapted *in situ* sampling by a microprobe to a microanalytical CE-ESI-MS

platform to enable the metabolic analysis of single cells in *X. laevis* embryos.[13, 23] This approach

allowed the detection of ~80 identified small polar metabolites and revealed quantitative

metabolic changes as single cells divide to form cell clones in the 8–32-cell embryo.[13] However,

microprobe CE-ESI-MS was restricted to cationic analysis due to frequent electrical breakdowns

that destabilized the electrospray in the negative ion mode (ESI–). Theoretically, the standard

metabolomics approach to perform independent analysis of cations and anions can deepen the

detectable portion of the single-cell metabolome. However, two-step metabolite extraction is

challenging or incompatible for single cells due to i) the limited amounts of material that are

available from a single cell and ii) cell heterogeneity hindering the use of multiple cells, even

from the same cell type, for sample processing.

Here, we addressed this technical limitation by enabling dual cationic-anionic

characterization of the same single identified cell in live embryos using CE-ESI-MS. Our

strategy (**Fig. 1**) extended microprobe single-cell sampling[13, 23] with essentially a one-pot

microextraction of cationic and anionic metabolites and also advanced CE-ESI-MS detection to

the negative ion mode (**Fig. 2**). For technology development and validation, the left-ventral (V1)

cell was used in 8-cell *X. laevis* embryos (see **Fig 1, left panel**), which is considerably large

(~500 μm in diameter, or ~65 nL in volume) to facilitate microprobe sampling and is readily

identifiable based on pigmentation, location, and in reference to established cell-fate maps[33-35, 38].

An ~10 nL volume of the identified cell, corresponding to ~5% of the total cell volume, was

withdrawn using a microfabricated capillary mounted to a three-axis translation stage following

our recent protocol.[13, 23] The aspirate was ejected into 4 μL of 40% aqueous acetonitrile

containing 40% methanol, which efficiently extracts small polar metabolites with different

physicochemical properties, including acidity and polarity.[20] The resulting extract, containing

cationic and anionic metabolites, thus raised a possibility for enhanced single-cell metabolomics

in the embryo.

Anionic analysis required extension of cationic CE-ESI-MS to separation and detection of

negatively charged metabolites. As an alternative to electron-scavenging reagents[39-43] or intricate

CE-ESI interface designs[28, 30, 32], we opted to refine our laboratory-built CE-ESI platform to

ensure stable electrospray operation in the negative ion mode. The setup, shown in **Figure 2A**,

builds on a co-axial sheath-flow interface that we[13, 20-23] and others[16-19, 44] extensively used for

cationic analysis and recently also nucleotide detection[28]. To minimize/eliminate electrical

discharges upon negative ion-mode ESI, we enclosed the CE-ESI emitter tip in a lab-fabricated

environmental chamber that was (optionally) purged with dry nitrogen gas at a controllable rate

and incident flow angle with respect to the electrospray emitter (see "N_2 bath gas"). The chamber was directly mounted on the atmospheric pressure interface of the mass spectrometer and featured a hole to allow fine-positioning of the CE-ESI emitter tip in the chamber in front of the orifice of the mass spectrometer inlet. Bidirectional illumination and a long-working distance stereomicroscope were implemented to monitor the stability of the electrospray.

The stability of the CE-ESI-MS system was evaluated. The electrohydrodynamic behavior of the liquid meniscus was monitored at the tip of the CE-ESI emitter using a stereomicroscope, while the temporal evolution of ion generation was followed using the mass spectrometer. The operational modality of the electrospray was identified according to established nomenclature (reviewed in Refs. [36, 45]) as follows (see examples in **Fig. 2A, right panel**): A stable Taylor-cone with axial spray emission marked the cone-jet regime; a pulsating liquid meniscus with axial spray emission indicated the burst, astable, or pulsing regimes; non-axial spray emission was categorized as "rim emission" in this study. Agreeing with earlier studies (see Ref. [18]), the CE-ESI interface yielded stable operation in the cone-jet regime under cationic experimental conditions (see **Experimental**) in air (no nitrogen bath gas used). Purging of the environmental chamber with a nitrogen bath gas (ambient temperature) at 0.4–1.0 L/min maintained stable operation with a variation of ~6% relative standard deviation (RSD) in total ion current (see **Fig. 2B, top panel**). Therefore, the CE-ESI setup equipped with the environmental chamber still maintained robust performance for cationic analysis in this study.

The modified CE-ESI setup was tuned for robust anionic analysis. Electrospray polarity switching from cationic measurement conditions destabilized spray generation (data not shown), which worsened upon replacement of the BGE with 20 mM bicarbonate, which was previously used for nucleotide analysis[28]. Encouraged by this study, we replaced the electrospray sheath

solution with 200 µM ammonium bicarbonate in 20%, 50%, and 70% isopropanol to test

electrospray stability in the negative ion mode. Although the temporal stability of ion generation

improved using a 50% isopropanol solution (**Fig. 2B, middle panel**), a ~39% RSD in the total

ion chromatogram (TIC) in our hand revealed still pronounced fluctuation for quantification.

Microscopy inspection of the emitter tip captured frequent transitions between the pulsating (data

not shown), rim (see **Fig. 2A right panel, middle inset**), and cone-jet electrospray regimes with

occasional electrical sparks between the emitter tip and the MS orifice plate (see **Fig. 2A right

panel, bottom inset**). These instabilities in electrostatic spraying and consequent ion generation

ceased upon continuous purging of the environmental chamber with a steady-stream of nitrogen

gas. After optimizing the nitrogen gas flow rate at 0.6 L/min and incidence perpendicularly to the

electrospray emitter (see **Fig. 2B**), the TIC stability was improved to only ~3% RSD variation.

The cationic and anionic separations provided complementary analytical performance for

detection. For several metabolite standards (e.g., creatine, lysine), quantification was tested

linear between ~100 nM and ~1 µM (regression coefficient, $R^2 > 0.99$) in both modalities, which

the digitizer of the mass spectrometer is expected to extend to an ~4-log-order dynamic range

following our recent study[22]. Based on the analysis of a 100 nM creatine standard, the lower limit

of detection was extrapolated to 7.5 nM (75 amol) during cationic and 5.5 nM (55 amol) during

anionic analysis. Furthermore, mass spectra resulting from anionic measurements contained

substantially fewer background ions, which also had lower ion intensities, suggesting minimized

spectral interferences compared to cationic analysis. **Figure 2B** exemplifies detection of the

pyridoxal anion at a ~3:1 analyte:background signal ratio (average ESI–) in a sparsely populated

spectrum, whereas the cation of this metabolite yielded a ~1:3 ratio in a complex mass spectrum.

These analytical figures of merits suggested a potential for sequential cationic and anionic

profiling of the same metabolite extract using the same CE-ESI-MS instrument, which we refer

to as "dual cationic-anionic" measurement in this report.

Dual Cationic-Anionic Metabolomics of Single Cells. We applied these methodologies to

characterize small metabolites in N = 4 single V1 cells (recall **Fig. 1**). As described earlier, an

~10 nL portion of the cell was aspirated *in situ* from a live 8-cell *X. laevis* embryo using a pulled

microcapillary. Small metabolites were extracted from the aspirate in 4 µL of 40% acetonitrile

containing 40% methanol. A ~10 nL portion of the resulting extract was analyzed under cationic

and then anionic conditions using the same CE-ESI-MS setup and different BGEs. Data-

dependent tandem MS was performed to facilitate metabolite identifications. These

measurements, thus, consumed a total of ~20 nL, viz. ~0.5% of metabolites that were extracted

from the V1 cell. Our recent findings using microsampling[13] suggests that microprobe CE-ESI-

MS with dual cationic-anionic analysis is scalable to smaller cells and later stages of the

developing embryo as well as other tissues and organisms.

These data provided rich metabolic information on the cell. After deisotoping and manual

annotation of the MS data, we found ~250 cationic and ~200 anionic nonredundant molecular

features between *m/z* 50–500. These numbers excluded non-covalent clusters as well as signals

that originated from the extraction solvents or the culturing media (e.g., polymers from vials and

salt peaks). These cationic molecular features agreed with our previous results.[13] A

comprehensive list of anionic molecular features is provided in **Supplementary Information

Table 1** (**Table S1**). Metabolite identifications were made for 60 cationic and 24 anionic

molecular features based on accurate mass, isotopic peak distribution analysis, tandem MS, and

comparison to MS-MS/MS data recorded on chemical standards, in our previous studies[13, 20-23],

or published in Metlin,[46] MzCloud (www.mzcloud.org), or the Human Metabolome Database

(HMDB)[2]. Metabolite identifications are tabulated for cations in **Table S2** and for anions in **Table S3**.

Cationic and anionic measurements complemented each other. There were noticeable differences between CE separation performance. **Figure 3** presents representative extracted ion electropherograms for a subset of identified metabolites from V1 cells. Although most metabolites were separated in a shorter amount of time during cationic analysis, anionic separation provided higher separation efficiency: The average number of theoretical plates (N) was 170,000 for cationic and 200,000 for anionic analyses. These separation performances compare favorably to other CE-ESI designs, including recent low-flow coaxial (N = 15,000 plates/m)[30] and sheathless (N = 40,000–60,000 plates/m)[32] porous tip sprayer with high-sensitivity detection. Additionally, metabolite identifications were also complementary (**Fig. 4**). Molecular assignments were made for 60 cations and 24 anions with 11 metabolites identified under both conditions (**Fig. 4A**). Detection performance was compared based on signal-to-noise (signal/noise) ratios that were calculated for these 11 metabolites (**Fig. 4B**). The results revealed similar sensitivity for alanine, glutamine, glutamic acid, lysine, and pyridoxal. Cationic analysis yielded higher sensitivity for arginine, creatine, guanine, and hypoxanthine, whereas anionic analysis was more sensitive for asparagine and aspartic acid. Therefore, differences in complementary separation performance and compound-dependent ionization translated into quantitative differences using the cationic and anionic methodologies.

The identified metabolites enabled pathway enrichment analysis. Metabolites that were identified by anionic, cationic, and dual anionic-cationic analyses were mapped to the KEGG metabolomic knowledgebase using MetaboAnalyst as the search engine (see details in **Experimental**). Pathway significance was calculated from pathway enrichment analysis, and

pathway impact was determined from pathway topology analysis. **Figure 5 (top panel)** plots

pathway significance vs. pathway impact from dual anionic-cationic analysis. Several pathways

were enriched to statistical significance ($p < 0.05$) with pathway impact varying between high

(>0.5), modest (0.2–0.5), and low (<0.2). Representative metabolic pathways are labeled in

Figure 5 (top panel). For example, arginine-proline and glycine-serine-threonine metabolism

were of high impact, whereas enrichment was modest for vitamin B6 metabolism and low for

glycero-phospholipid metabolism.

Furthermore, anionic and cationic analyses provided complementary information for

pathway analysis. **Table 1** compares pathway enrichment and pathway impact based on

metabolites that were identified during the cationic, anionic, and dual cationic-anionic

measurements. Cationic and anionic analyses appeared to cover several pathways of high impact,

including alanine-aspartate-glutamate, arginine-proline, and glutamine-glutamate. The

complementarity of cationic and anionic detection is illustrated for the arginine-proline pathway

in **Figure 5 (bottom panel)**. Notably, additional metabolite identifications that resulted from

dual cationic-anionic analysis helped improve statistical significance and/or pathway impact for

several pathways, including glycerophospholipid and vitamin B6 metabolism (see **Table 1**).

Combined, these results suggest that dual cationic-anionic analysis by microprobe single-cell

CE-ESI-MS has the potential to provide deeper coverage of metabolism than feasible by these

approaches in isolation.

CONCLUSIONS

In this study, we advanced CE-ESI-MS technology to enable dual cationic-anionic analysis

of metabolites in single embryonic cells. *In situ* microprobe sampling using a microfabricated

capillary allowed us to sample an identified cell directly in a live *X. laevis* embryo under optical guidance by a stereomicroscope. To analyze metabolites extracted from the collected cell content, we equipped an in-house built CE-ESI-MS[22] platform with dual capability to perform cationic and anionic analysis using different BGEs for separation, without modifying the setup between sequential measurements. Optimization of experimental variables and the use of a nitrogen bath gas to minimize/eliminate electrical breakdown upon negative electrospray ensured sufficiently reproducible and robust operation for single-cell investigations in trace sensitivity (~5 nM, viz. ~50 amol demonstrated here).

The approach affords analytical benefits for biological studies on single cells. *In situ* microprobe sampling is compatible with complex tissues and organisms, as we demonstrated for 8-cell embryos of *X. laevis* in this work. CE-ESI-MS consumes sufficiently small amounts of extracts to afford multiple analysis of the same extract under cationic and anionic conditions. With complementary performance, the metadata resulting from these approaches improved metabolite identifications and quantification, which in turn led to better coverage of metabolic networks in single cells. This study design complements earlier works in which bare fused or coated capillaries were used to deepen metabolic coverage. Further improvements in detection sensitivity and expansion of metabolomic MS–MS/MS databases are needed to help identification of molecular features that were detectable from the single cells. Combined, results from this study and recent works[13, 19, 22, 28] suggest that dual cationic and anionic microprobe CE-ESI-MS is scalable to smaller cells and other types of cells and organisms to understand cell biology at the level of small molecules: the metabolome.

TABLES

Table 1. KEGG pathway analysis (statistical p-value and pathway impact) for metabolites identified in single V1 cells by microprobe CE-ESI-MS. The number of metabolites that participate in canonical networks ("Total") and identified in this study ("Hits") are shown.

| Name of Metabolic Pathway	Total	Cationic Analysis			Anionic Analysis			Dual Analysis		
		Hits	p	Impact	Hits	p	Impact	Hits	p	Impact
Alanine, aspartate, glutamate	24	7	1.06E-05	0.74	5	3.24E-05	0.60	7	4.34E-05	0.74
Arginine, proline	43	12	7.33E-09	0.54	7	3.57E-06	0.23	13	8.17E-09	0.54
Glutamine, glutamate	5	2	1.12E-02	1.00	2	2.27E-03	1.00	2	1.75E-02	1.00
Glutathione	26	7	1.91E-05	0.46	1	0.36	0.03	7	7.69E-05	0.46
Glycero-phospholipid	28	2	0.265	0.03	2	0.081	0.06	4	0.032	0.09
Glycine, serine, threonine	31	7	6.66E-05	0.57	2	0.10	0.00	8	3.14E-05	0.57
Histidine	14	4	1.12E-3	0.24	2	2.26E-02	0.00	4	2.25E-03	0.24
Nitrogen	9	4	1.61E-4	0.00	2	9.45E-3	0.00	4	3.64e-4	0.00
Phenylalanine, tyrosine, tryptophan	4	2	7.21E-03	1.00	0	0	0.00	2	7.21E-03	1.00
Valine, leucine, isoleucine	13	4	8.21E-04	1.00	0	0	0.00	4	8.21E-04	1.00
Vitamin B6	9	1	0.281	0.49	1	0.145	0.00	2	0.056	0.49

FIGURES
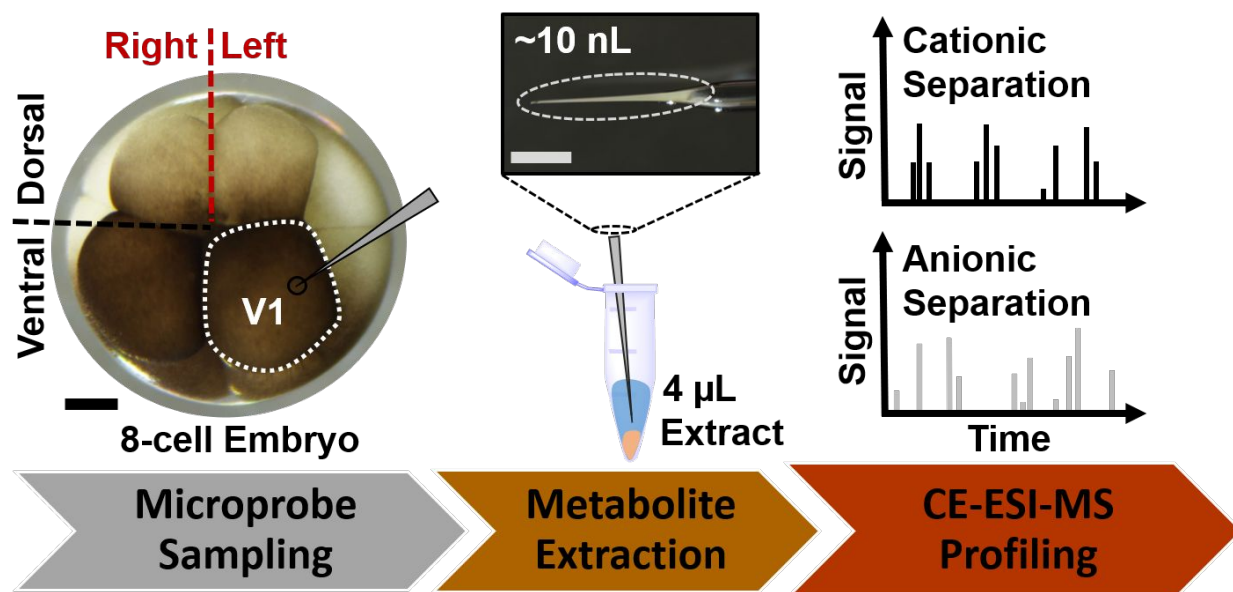
Figure 1. Microprobe CE-ESI-MS strategy to measure cationic and anionic metabolites from the

same identified cell in a live *X. laevis* embryo. Shown here, the left animal-ventral (V1) cell of

the 8-cell embryo was identified, and ~10 nL of its content was aspirated for one-pot metabolite

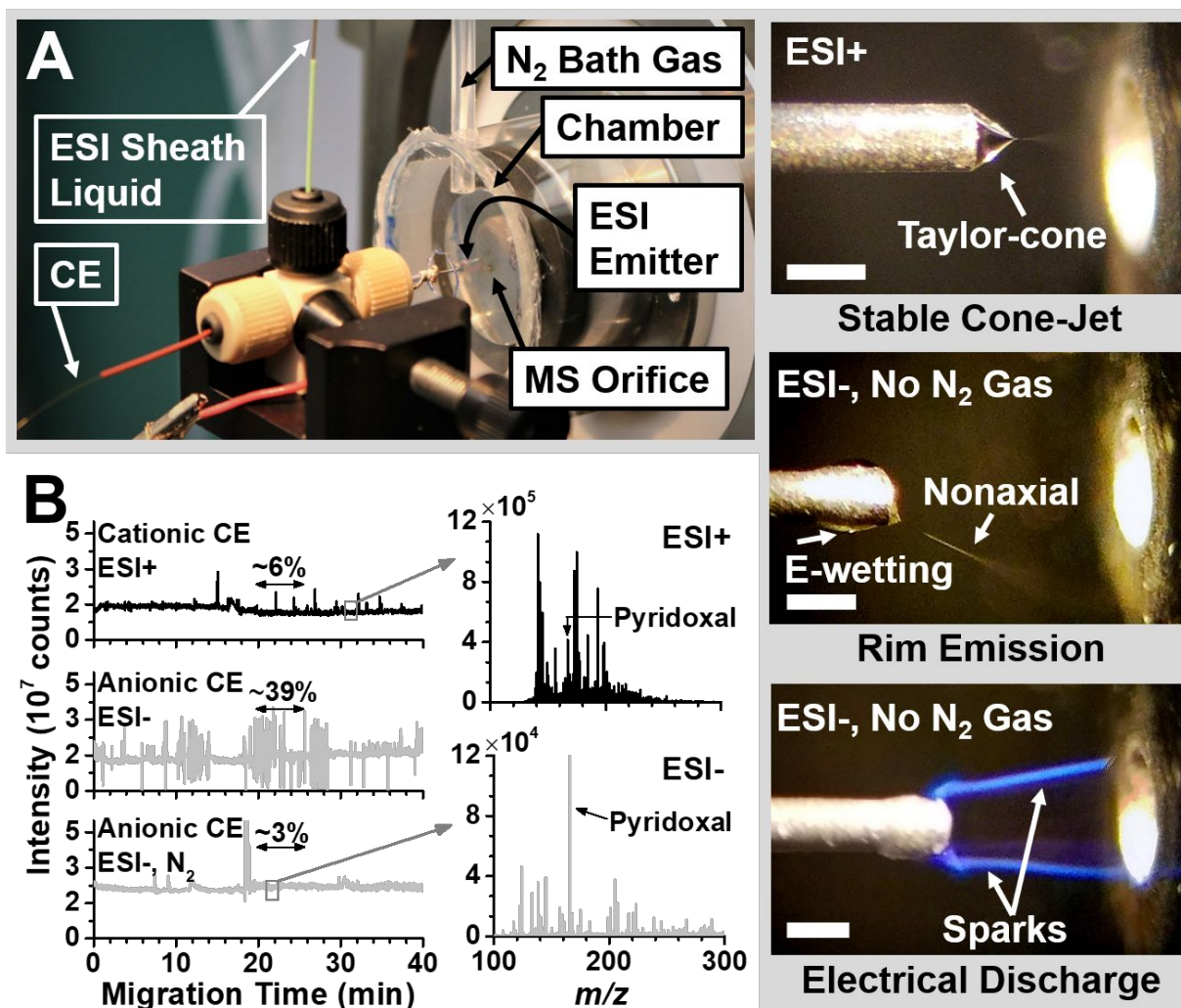extraction, followed by cationic and anionic profiling of the same cell extract. Scale bars = 250

µm.

Figure 2. CE-ESI-MS for cationic and anionic analysis. **(A)** The CE-ESI-MS interface with

major components labeled. Microscopy comparison of stable Taylor-cone in ESI+ (top panel)

and nonaxial (rim) emission (middle panel) and electrical discharge (spark) in ESI– without

nitrogen bath gas. **(B)** Total ion chromatograms revealing stable operation during cationic

separation with ESI+ (top panel). Astable ESI– with anionic separation (middle panel) was

stabilized upon enclosing the electrospray emitter in a nitrogen-filled environmental chamber

(bottom panel). Spray stability is quantified as % relative standard deviation (RSD).

Representative mass spectra revealing simplified chemical background during ESI–.
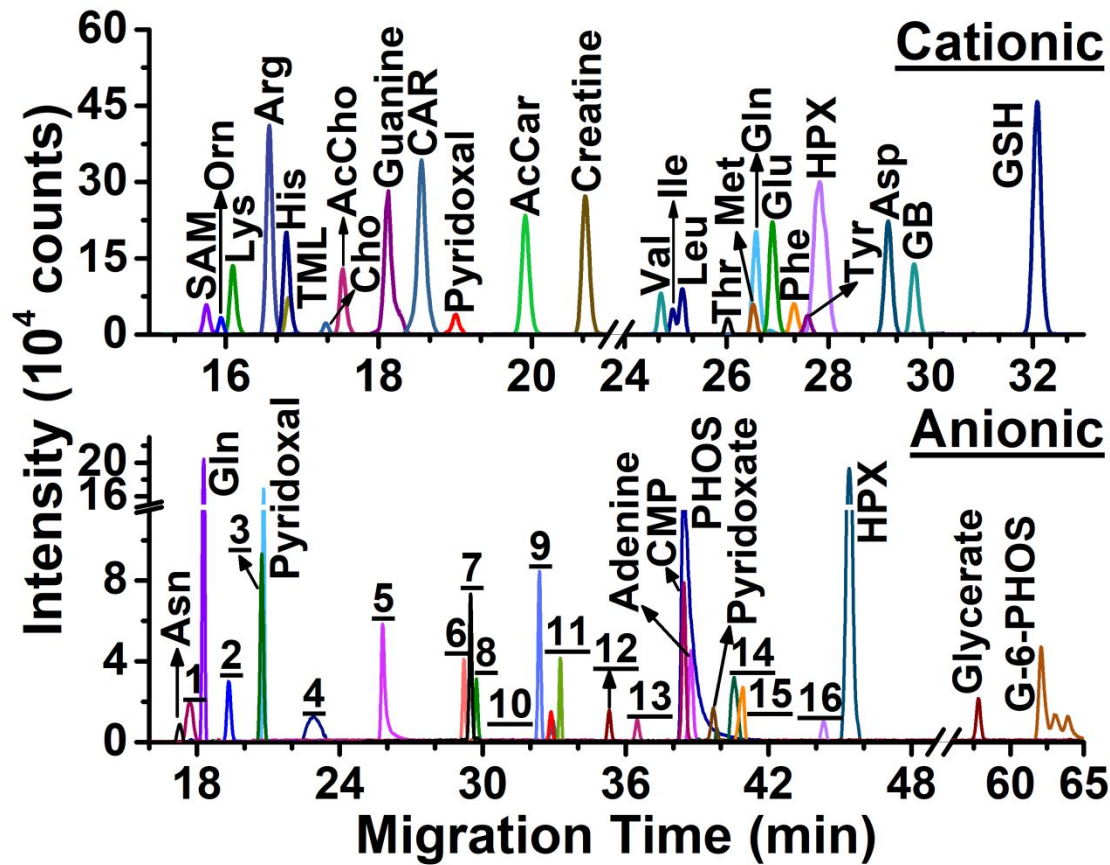
Figure 3. Cationic and anionic profiling of metabolites in the same V1 cell in a live *X. laevis* embryo. Representative selected ion electropherograms are shown for select signals. Identified metabolites are labeled (see abbreviations in **Tables S2–3**). Numbers correspond to molecular features in **Table S4**.
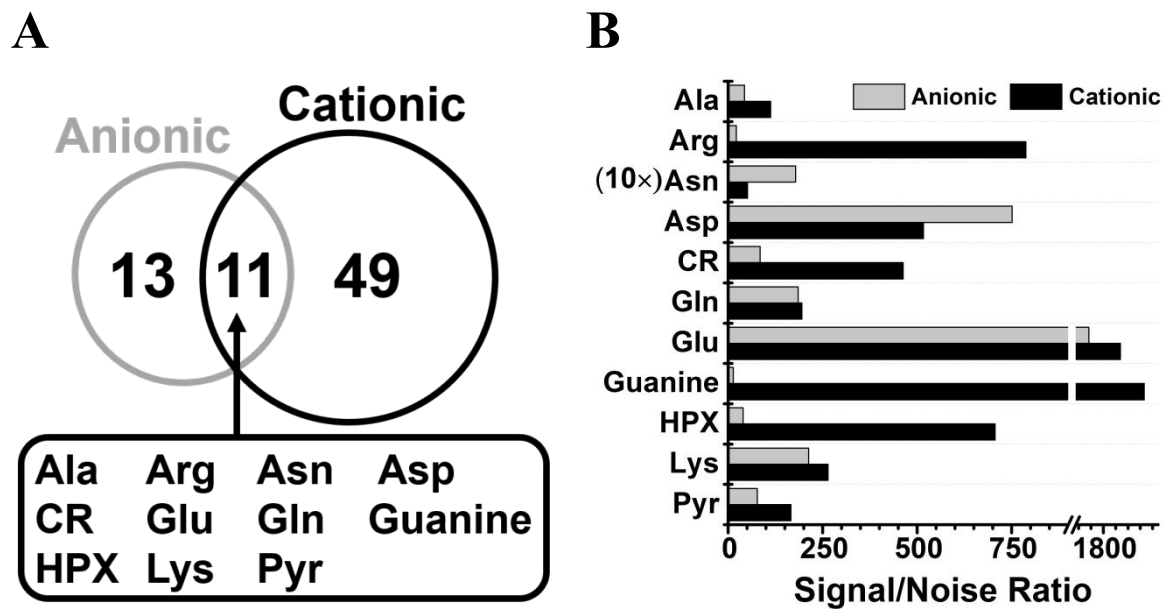
A

B

Figure 4. Complementary **A)** identification and **B)** quantification of metabolites in single

Xenopus laevis V1 cells using dual cationic-anionic microprobe CE-ESI-MS. Key: Cr, creatine;
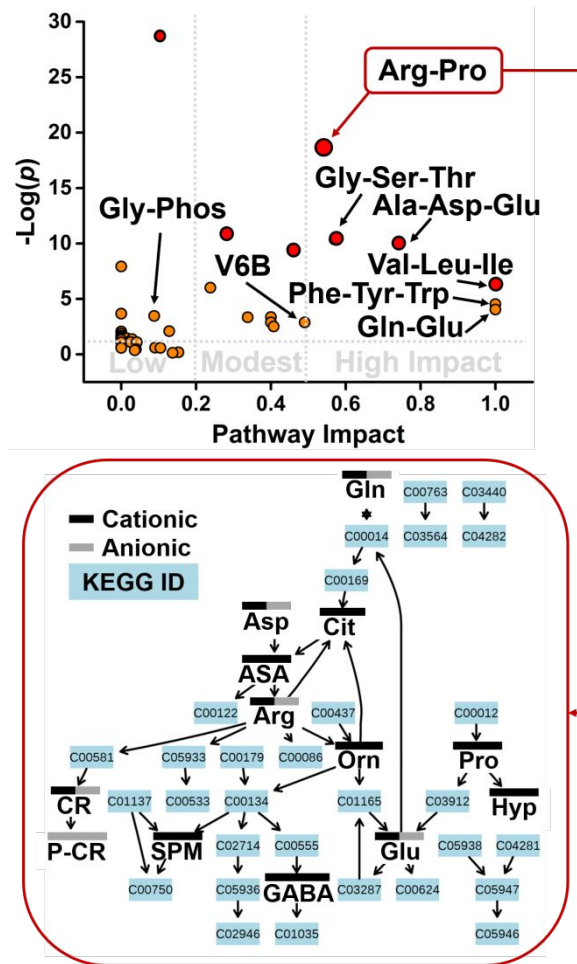
HPX, hypoxanthine; Pyr, pyridoxal.

Figure 5. KEGG pathway analysis for metabolites identified in single V1 cells. Values of

statistical significance (*p*) and impact are shown for labeled pathways in **Table 1**. Pathway view

for arginine-proline metabolism marking complementary detection by cationic and anionic

analyses. Key: ASA, argininosuccinate; Cit, citrulline; CR, creatine; Gly-Phos, Glycero-

phospholipid metabolism; Hyp, hydroxyproline; P-CR, phosphocreatine; SPM, spermidine; V6B,

vitamin 6B metabolism.

1
2
3
4
5
6
7
8
9
10
11
12
13
14
15
16
17
18
19
20
21
22
23
24
25
26
27
28
29
30
31
32
33
34
35
36
37
38
39
40
41
42
43
44
45
46
47
48
49
50
51
52
53
54
55
56
57
58
59
60

REFERENCES

1.   R. Zenobi, *Science*, 2013, **342**, 1243259.
2.   D. S. Wishart, Y. D. Feunang, A. Marcu, A. C. Guo, K. Liang, R. Vazquez-Fresno, T. Sajed, D. Johnson, C. Li, N. Karu, Z. Sayeeda, E. Lo, N. Assempour, M. Berjanskii, S. Singhal, D. Arndt, Y. Liang, H. Badran, J. Grant, A. Serra-Cayuela, Y. Liu, R. Mandal, V. Neveu, A. Pon, C. Knox, M. Wilson, C. Manach and A. Scalbert, *Nucleic Acids Res.*, 2018, **46**, D608-D617.
3.   H. L. Sive, R. M. Grainger and R. M. Harland, *Early development of Xenopus laevis : a laboratory manual*, Cold Spring Harbor Laboratory Press, Cold Spring Harbor, N.Y., 2000.
4.   T. Acunha, C. Simo, C. Ibanez, A. Gallardo and A. Cifuentes, *J. Chromatogr. A*, 2016, **1428**, 326-335.
5.   S. S. Rubakhin, E. V. Romanova, P. Nemes and J. V. Sweedler, *Nat. Methods*, 2011, **8**, S20-S29.
6.   S. S. Rubakhin, E. J. Lanni and J. V. Sweedler, *Curr. Opin. Biotechnol.*, 2013, **24**, 95-104.
7.   Y. Y. Yang, Y. Y. Huang, J. H. Wu, N. Liu, J. W. Deng and T. G. Luan, *Trends Anal. Chem.*, 2017, **90**, 14-26.
8.   T. J. Comi, T. D. Do, S. S. Rubakhin and J. V. Sweedler, *J. Am. Chem. Soc.*, 2017, **139**, 3920-3929.
9.   L. Yin, Z. Zhang, Y. Liu, Y. Gao and J. Gu, *Analyst*, 2018, Accepted Manuscript
10.   M. K. Passarelli and A. G. Ewing, *Curr. Opin. Chem. Biol.*, 2013, **17**, 854-859.
11.   R. M. Liu, N. Pan, Y. L. Zhu and Z. B. Yang, *Anal. Chem.*, 2018, **90**, 11078-11085.
12.   A. Saha-Shah, C. M. Green, D. H. Abraham and L. A. Baker, *Analyst*, 2016, **141**, 1958-1965.
13.   R. M. Onjiko, E. P. Portero, S. A. Moody and P. Nemes, *Anal. Chem.*, 2017, **89**, 7069-7076.
14.   S. A. Stopka, R. Khattar, B. J. Agtuca, C. R. Anderton, L. Pasa-Tolic, G. Stacey and A. Vertes, *Front. Plant Sci.*, 2018, **9**, 1646.
15.   T. J. Comi, M. A. Makurath, M. C. Philip, S. S. Rubakhin and J. V. Sweedler, *Anal. Chem.*, 2017, **89**, 7765-7772.
16.   T. Lapainis, S. S. Rubakhin and J. V. Sweedler, *Anal. Chem.*, 2009, **81**, 5858-5864.
17.   P. Nemes, A. M. Knolhoff, S. S. Rubakhin and J. V. Sweedler, *Anal. Chem.*, 2011, **83**, 6810-6817.
18.   P. Nemes, S. S. Rubakhin, J. T. Aerts and J. V. Sweedler, *Nat. Protoc.*, 2013, **8**, 783-799.
19.   J. T. Aerts, K. R. Louis, S. R. Crandall, G. Govindaiah, C. L. Cox and J. V. Sweedler, *Anal. Chem.*, 2014, **86**, 3203-3208.
20.   R. M. Onjiko, S. E. Morris, S. A. Moody and P. Nemes, *Analyst*, 2016, **141**, 3648-3656.
21.   R. M. Onjiko, D. O. Plotnick, S. A. Moody and P. Nemes, *Anal. Methods*, 2017, **9**, 4964-4970.
22.   R. M. Onjiko, S. A. Moody and P. Nemes, *Proc. Natl. Acad. Sci. U. S. A.*, 2015, **112**, 6545-6550.
23.   R. M. Onjiko, E. P. Portero, S. A. Moody and P. Nemes, *J. Vis. Exp.*, 2017, DOI: 10.3791/56956, e56956.
24.   R. Ramautar, G. W. Somsen and G. J. de Jong, *Electrophoresis*, 2013, **34**, 86-98.

24

25. R. Ramautar, G. W. Somsen and G. J. de Jong, *Electrophoresis*, 2017, **38**, 190-202.
26. R. Ramautar, G. W. Somsen and G. J. de Jong, *Electrophoresis*, 2015, **36**, 212-224.
27. R. L. C. Voeten, I. K. Ventouri, R. Haselberg and G. W. Somsen, *Anal. Chem.*, 2018, **90**, 1464-1481.
28. J. X. Liu, J. T. Aerts, S. S. Rubakhin, X. X. Zhang and J. V. Sweedler, *Analyst*, 2014, **139**, 5835-5842.
29. T. Soga, K. Igarashi, C. Ito, K. Mizobuchi, H. P. Zimmermann and M. Tomita, *Anal. Chem.*, 2009, **81**, 6165-6174.
30. S. A. Sarver, N. M. Schiavone, J. Arceo, E. H. Peuchen, Z. Zhang, L. Sun and N. J. Dovichi, *Talanta*, 2017, **165**, 522-525.
31. L. Lin, X. Liu, F. Zhang, L. Chi, I. J. Amster, F. E. Leach, 3rd, Q. Xia and R. J. Linhardt, *Anal. Bioanal. Chem.*, 2017, **409**, 411-420.
32. M. C. Gulersonmez, S. Lock, T. Hankemeier and R. Ramautar, *Electrophoresis*, 2016, **37**, 1007-1014.
33. S. A. Moody, *Methods Mol. Biol.*, 2000, **135**, 331-347.
34. S. L. Klein, *Dev. Biol.*, 1987, **120**, 299-304.
35. S. A. Moody and M. J. Kline, *Anat. Embryol.*, 1990, **182**, 347-362.
36. P. Nemes, I. Marginean and A. Vertes, *Anal. Chem.*, 2007, **79**, 3105-3116.
37. J. Chong, O. Soufan, C. Li, I. Caraus, S. Li, G. Bourque, D. S. Wishart and J. Xia, *Nucleic Acids Res.*, 2018, **46**, W486-W494.
38. S. A. Moody, *Dev. Biol.*, 1987, **119**, 560-578.
39. R. F. Straub and R. D. Voyksner, *J. Am. Soc. Mass Spectrom.*, 1993, **4**, 578-587.
40. M. G. Ikonomou, A. T. Blades and P. Kebarle, *J. Am. Soc. Mass Spectrom.*, 1991, **2**, 497-505.
41. R. B. Cole and A. K. Harrata, *J. Am. Soc. Mass Spectrom.*, 1993, **4**, 546-556.
42. P. J. McClory and K. Håkansson, *Anal. Chem.*, 2017, **89**, 10188-10193.
43. Z. Wu, W. Gao, M. A. Phelps, D. Wu, D. D. Miller and J. T. Dalton, *Anal. Chem.*, 2004, **76**, 839-847.
44. A. M. Knolhoff, K. M. Nautiyal, P. Nemes, S. Kalachikov, I. Morozova, R. Silver and J. V. Sweedler, *Anal. Chem.*, 2013, **85**, 3136-3143.
45. I. Marginean, P. Nemes and A. Vertes, *Phys. Rev. E*, 2007, **76**, 026320.
46. C. Guijas, J. R. Montenegro-Burke, X. Domingo-Almenara, A. Palermo, B. Warth, G. Hermann, G. Koellensperger, T. Huan, W. Uritboonthai, A. E. Aisporna, D. W. Wolan, M. E. Spilker, H. P. Benton and G. Siuzdak, *Anal. Chem.*, 2018, **90**, 3156-3164.